ELSEVIER

Inorganica Chimica Acta 229 (1995) 229–239

Inorganica Chimica Acta

Protein-bound iron–sulfur clusters: application of a structural database ☆

Jeffrey R. Long, R.H. Holm *

Department of Chemistry, Harvard University, Cambridge, MA 02138, USA

Received 16 June 1994; revised 22 August 1994

Abstract

A recently developed database is employed in supplying structural models for potential new protein-bound iron–sulfur clusters. The database consists of edge-sharing tetrahedra-based clusters generated from fragments of a parent solid with the antifluorite structure. (Appropriate pieces of the solid are converted into terminally ligated $Fe_mS_qL_l$ clusters and subjected to a variety of structural rearrangements.) A protein-bound subset comprised of clusters with chemical formulae $Fe_mS_{m-1}L_l$, $Fe_mS_mL_l$ and $Fe_mS_{m+1}L_l$ is extracted from the database, and enumerated for $m \leqslant 8$. This subset embodies an extensive array of cluster structures, all reasonable candidates for potential iron–sulfur clusters in biology. Clusters with sulfur bridging modalities of four or less, and containing one or fewer associated terminal ligands per iron atom are considered the most likely candidates. Over fifty of these structures are illustrated for detailed examination. It is proposed that the protein-bound subset described herein may be utilized as a source of structural models for testing during crystal structure determination for proteins containing novel iron–sulfur clusters. In a further application, stripping the outer ligands, L, from subset clusters provides a collection of possible structures for the series of laser ablated cluster ions $[Fe_mS_{m-1}]^-$, $[Fe_mS_m]^-$ and $[Fe_mS_{m+1}]^-$. These are also enumerated for nuclearities, m, of eight or less.

Keywords: Iron–sulfur clusters; Iron–sulfur proteins; Structural database

1. Introduction

Over the last twenty years, the field of iron–sulfur biochemistry has become firmly established. The structure and function of iron–sulfur centers of varying nuclearities in proteins and enzymes continues to evolve as a significant area for investigation [1]. Essential to this research endeavor is a detailed structural knowledge of the biomolecule, including its iron–sulfur mononuclear and cluster components. To date, X-ray crystallographic studies have provided the most detailed and reliable sources of information. However, the resolution achieved by this technique is not necessarily sufficient for direct structure determination of the comparatively small metal clusters, including atom connectivities. In such cases, a typical recourse is to propose a number of models for the cluster structure, attempting to fit the observed electron density. To facilitate this process, and reduce the risk of overlooking reasonable (and possibly correct) structures, we herein provide an exhaustive database of structural models for potential new clusters in iron–sulfur biochemistry.

As detailed in Table 1 [2–34], iron–sulfur clusters found in crystallographically resolved proteins exhibit several recurrent structures. These are collected in Fig. 1. The simplest, **1**, consists of a rhombic Fe_2S_2 core in which each iron atom is terminally coordinated by two cysteinate sulfur atoms. The idealized stereochemistry at the iron sites in all clusters with terminal cysteinate ligands is tetrahedral. The cubane core of **3** pervades much of iron–sulfur cluster chemistry, and derives from an Fe_4 tetrahedron, each face of which is capped by a sulfur atom to form a distorted Fe_4S_4 cube. Cluster **4**, a [1:3] site-differentiated version of **3**, serves as the catalytic site of the enzyme aconitase; here cysteinate ligation is replaced by water or hydroxide at the iron atom to which the substrate binds. Formal removal of one iron atom from the cubane core yields a cuboidal Fe_3S_4 core, as present in cluster **2**. Two distinct octanuclear clusters reside in nitrogenase proteins, and these have only recently been resolved structurally. The 'P-cluster' of nitrogenase reportedly consists of two cubanes joined via two cysteinate bridges and

☆ This paper is dedicated to Professor F.A. Cotton on the occasion of his 65th birthday.

* Corresponding author.

SSDI 0020-1693(94)04249-U

Table 1
X-ray structural determinations of iron–sulfur proteins [a] containing Fe_2S_2, Fe_3S_4 and Fe_4S_4 clusters

Protein	Cluster		Resolution (Å)	Ref.
Spirulina platensis Fd	$[Fe_2S_2]^{2+}$	(1)	2.5	[2–4]
Aphanothece sacrum Fd	$[Fe_2S_2]^{2+}$	(1)	2.2	[5]
Halobacterium Fd	$[Fe_2S_2]^{2+}$	(1)	3.2	[6,7]
Anabaena 7120 Fd vegetative	$[Fe_2S_2]^{2+}$	(1)	2.5	[8,9]
heterocyst	$[Fe_2S_2]^{2+}$	(1)	1.7	[9,10]
Aconitase (beef heart mitochondrial)	$[Fe_3S_4]^{1+}$	(2)	2.1	[11]
Desulfovibrio gigas Fd II	$[Fe_3S_4]^{1+}$	(2)	1.7	[12,13]
Azotobacter vinelandii Fd I	$[Fe_3S_4]^{1+}$	(2)	2.7–1.9	[14–18]
Chromatium vinosum Fd	$[Fe_4S_4]^{2+,1+}$	(3)	2.0	[19–21]
Bacillus thermoproteolyticus Fd	$[Fe_4S_4]^{2+}$	(3)	2.3	[22]
E. coli Endonuclease III	$[Fe_4S_4]^{2+}$	(3)	2.0	[23]
Ectothiorhodospira halophilia Fd	$[Fe_4S_4]^{2+}$	(3)	2.5	[24]
W3A1 trimethylamine dehydrogenase	$[Fe_4S_4]^{2+}$	(3)	2.4	[25]
Rhodocyclus tenuis Fd	$[Fe_4S_4]^{2+}$	(3)	1.5	[26]
Peptococcus aerogenes Fd	$2[Fe_4S_4]^{2+}$	(3)	2.8, 2.0	[27,28]
Azotobacter vinelandii Fd I	$[Fe_4S_4]^{2+}$	(3)	2.7–1.9	[14–18]
Ectothiorhodospira vacuolata Fd	$[Fe_4S_4]^{2+}$	(3)	1.8	[29]
Aconitase (beef heart mitochondrial)	$[Fe_4S_4]^{2+}$	(4)	2.5	[30]
Azotobacter vinelandii Fe protein [b]	$[Fe_4S_4]^{2+}$	(4)	2.9	[31]
Azotobacter vinelandii FeMo protein [b]	$[Fe_8S_8]$	(5)	2.7, 2.2	[32,33]
Clostridium pasteurianum FeMo protein [b]	$[Fe_8S_8]$	(5)	3.0	[34]

[a] Generically, many iron–sulfur proteins are referred to as ferredoxins (Fds).
[b] Nitrogenase proteins.

an intercubane S–S bond, as shown in **5** [32–34]. The latest result, however, indicates a closely related structure in which the persulfide unit is replaced by a single μ_6-S atom [35]. The cofactor of nitrogenase [36,37], is an even more complex iron–sulfur cluster, which also contains one molybdenum (or vanadium) atom in a completely unprecedented structure, **6**. Its $MoFe_7S_9$ core is made up of Fe_4S_3 and $MoFe_3S_3$ cuboidal fragments (with the metal:sulfur population the inverse of **2**) joined by three μ_2-S atom bridges. Equivalently, **6** may be described as an Fe_6 trigonal prism with nine edge-bridging sulfurs, capped at one end by a cysteinate-bound iron, and at the other by a molybdenum atom coordinated by a bidentate homocitrate and the imidazole group of a histidyl residue.

Numerous synthetic analogues $[Fe_2S_2(SR)_4]^{2-}$ and $[Fe_4S_4(SR)_4]^{1-,2-,3-}$ of protein clusters **1** and **3** have been prepared and their properties (including detailed structural analyses) elucidated in considerable detail [38,39]. In these and other analogues, thiolate simulates cysteinate binding. The chemistry of [1:3] site-differentiated Fe_4S_4 clusters similar to **4** has been developed more recently [40,41]. An analogue of cuboidal cluster **2** has not yet been isolated in substance. However, a core isomer has been prepared in the form of the linear cluster $[Fe_3S_4(SR)_4]^{3-}$ (**7**) [42].

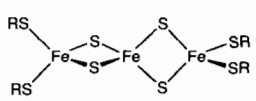

7

The inactive form of aconitase contains **2**; when the enzyme structure is unfolded, the cuboidal cluster rearranges into **7** (R = Cys) [43,44], as identified by spectroscopic comparison with an authentic cluster. This linear isomer has not been detected in any other protein. No analogue of **5** has been prepared. The cofactor **6** presents a complicated problem in cluster synthesis. Synthetic cuboidal Fe_4S_3 fragments have been structurally characterized [45–48], including cases in which the unique iron atom is terminally ligated by thiolate [48]. Heterometal cuboidal MFe_3S_3 clusters have not been prepared, but there are many examples of cubane-type MFe_3S_4 clusters [45,49,50]. These may be considered as structural parents of the cuboidal Fe_3S_4 species. Protein-bound clusters of this type have been produced by the reaction of cuboidal unit **2** with extrinsic metal ions [45], and, in several cases, their structures have been proven via comparison with structurally established synthetic counterparts [51]. As yet, no MFe_3S_4 cluster has been encountered in a *native* protein.

In addition to the now-standard Fe_2S_2, Fe_3S_4 and Fe_4S_4 cores present in protein-bound clusters **1–5** and their synthetic analogues, evidence is mounting in support of the existence of other types of iron–sulfur clusters in biology. Nearly all iron-only hydrogenases [52–56] contain a unique catalytic site, the 'H-cluster', which appears to be comprised of 3–6 iron atoms, with significant non-cysteinate (nitrogen) ligation in at least one case [53]. The site in oxidized enzymes has an $S = 1/2$ ground state and a rhombic EPR spectrum. For no enzyme has the Fe:S ratio of its H-cluster been

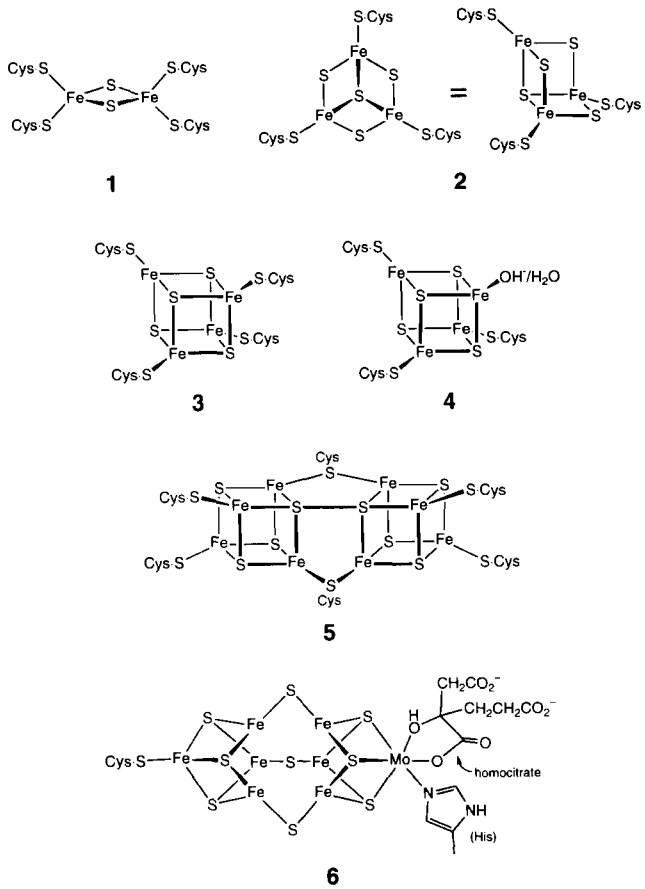

Fig. 1. Crystallographically resolved clusters in iron-sulfur proteins: rhombic (**1**), trinuclear cuboidal (**2**), cubane (**3**), [1:3] site-differentiated cubane (**4**), P-cluster (**5**) and FeMo-cofactor (**6**). In a more recent P-cluster structure, the two four-coordinate S atoms of **5** are fused into one μ_6-S atom (see **57** below).

established. A 50 kDa protein isolated from *Desulfovibrio vulgaris* (Hildenborough) contains six iron atoms [57,58]. Comparison of its $S = 1/2$ EPR spectrum with those of the prismane clusters $[Fe_6S_6L_6]^{3-}$ ($L = RS^-$, Cl^-) has raised the possibility that the protein-bound cluster may have the same or similar stereochemistry as the synthetic prismanes [59,60]. A 57 kDa protein with the atom ratio Fe:S ≈ 1 recently isolated from *Desulfovibrio desulfuricans* has been deduced to contain two six-iron clusters [61]. One of these when reduced exhibits an $S = 1/2$ EPR spectrum similar to the prismanes whereas the other, from Mössbauer and EPR spectroscopic evidence, has mixed terminal ligands with coordination numbers exceeding 4 at some iron sites and an $S = 9/2$ ground state. No function has yet been established for the proteins from these *Desulfovibrio* bacteria. Putative $S = 9/2$ Fe–S clusters of unknown composition have also been claimed in the dissimilatory sulfite reductase of *Desulfovibrio vulgaris* (Hildenborough) [62] and the carbon monoxide dehydrogenase of *Methanothrix soehngenii* [63]. These incompletely defined clusters demonstrate, at the very least, that new iron–sulfur clusters await discovery and characterization. They reinforce the desirability, if not the requirement, of a complete set of rational structures for clusters of a given nuclearity.

While we emphasize here the biological significance of iron–sulfur arrays **1–5** and shall deal with other possible structures of protein-bound clusters, this family represents only a segment from a vast range of structures displayed in metal–chalcogenide cluster compounds [45,49,50,64–74]. The recent treatment of the subject by Dance and Fisher [74] exposes this enormous structural diversity inherent to molecular metal chalcogenides.

2. Generation of an iron–sulfur cluster database

In this section, we outline the methods employed in generating a comprehensive structural database of iron–sulfur clusters. The entire process, along with a general strategy for creating such a construct, is described elsewhere in full detail [75]. This approach has practical advantages over previous approaches in its ability to produce immediately accessible structures with tailored atom stereochemistries. A particularly relevant example of a previous approach wherein connectivities are enumerated for metal–chalcogenide clusters containing four-coordinate metal centers may be found in Ref. [76].

As with any enumerative effort, it is first necessary to delimit the rules which govern the set. Based on previously observed synthetic and biological examples, the iron–sulfur cluster family will be confined to clusters $Fe_mS_qL_l$ composed of edge-sharing FeX_4 (X = S, L) tetrahedra, where L is a monodentate terminal ligand. This definitive structural criterion is employed in the design of a parent solid: the simple motif of edge-sharing FeS_4 tetrahedra is propagated in all three dimensions to yield an infinitely extended solid. The product is a fictitious solid of formula Fe_2S which adopts the antifluorite structure (Fig. 2), wherein each iron-centered tetrahedron shares all six of its edges with neighboring tetrahedra. As a parent solid, this structure serves as a source of iron–sulfur clusters in the form of edge-sharing tetrahedra-based fragments. Its aptitude for such a role is made evident by numerous synthetic clusters with structures clearly related to antifluorite fragments, including the clusters $[Fe_8S_6I_8]^{2-,3-,4-}$ [77–79] which display a structure (see **10** in Fig. 3) featuring the exact contents of the unit cell outlined in Fig. 2.

Computer generation of appropriate antifluorite fragments is facilitated by utilizing a graph representation of chemical structure. In this simplification of the parent antifluorite structure, each FeS_4 tetrahedron is replaced by a point, and an edge shared between two tetrahedra is represented by a line connecting the corresponding

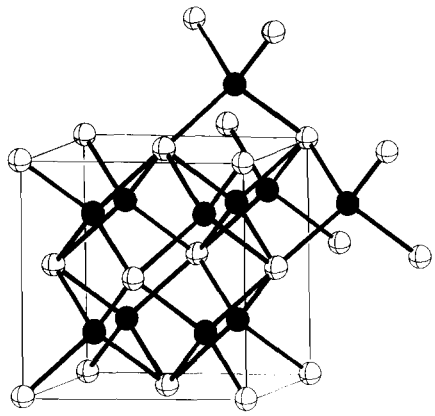

Fig. 2. Unit cell of the Fe_2S parent solid. This is simply the antifluorite structure, consisting of an fcc lattice of S atoms (white spheres) with Fe atoms (black spheres) occupying all of the tetrahedral holes. Each sulfur is coordinated by eight iron atoms in a cubic arrangement.

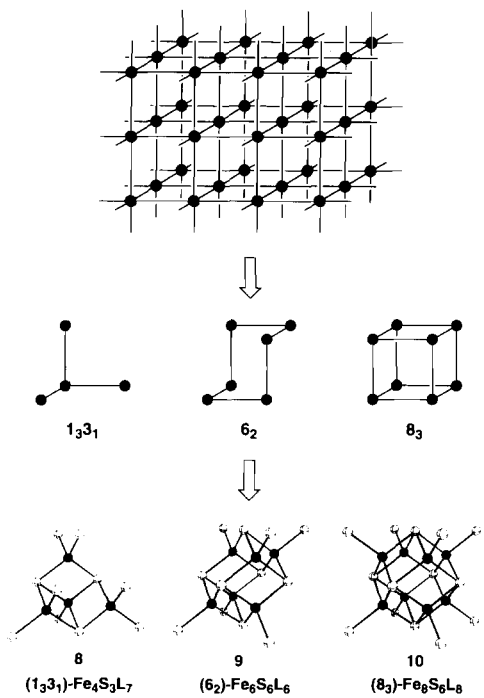

Fig. 3. The fragment generation process. Beginning with a simple cubic lattice representing the antifluorite parent solid (top), lattice animals are generated (middle), and subsequently transformed into edge-sharing tetrahedral iron–sulfur clusters (bottom). Animals and clusters are labeled by their respective degree partitioning and reduced PCP notations.

points. The result is a simple cubic lattice of points and lines, as shown at the top in Fig. 3. Note that each point is connected to six neighboring points, just as each tetrahedron shares its six edges with neighboring tetrahedra in the antifluorite structure. All of the connected graphs, or *animals*, indigenous to this lattice are generated by a straightforward recursive procedure. Animals containing m points are constructed by adding a point in all possible ways to each animal containing m-1 points, and eliminating duplicates. Three examples are depicted in the middle of Fig. 3. Accompanying each animal is a descriptive notation in which the number of points m is partitioned by degree (shown in subscript). (The degree of a point is the number of lines incident with it.) For example, the leftmost animal has descriptor $1_3 3_1$, indicating that it contains one point of degree three (1_3) and three points of degree one (3_1). Animals are converted into antifluorite fragments by replacing each point with an iron atom and its associated tetrahedron of sulfur atoms. Terminal sulfur atoms are relabeled as generic monodentate ligands, L, yielding a complete set of antifluorite 'fragment' cluster $Fe_mS_qL_l$. These clusters form the basis for our iron–sulfur cluster database, and are enumerated by nuclearity (m) in Table 2. The close relationship between corresponding animals and clusters is apparent from the examples in Fig. 3. The graph descriptor is retained as a prefix to the cluster formula in a reduced polyhedra connectivity partitioning (PCP) notation [75] indicating the distribution of iron-centered tetrahedra by the number of edges they share. For present purposes, the notation is included merely as an aid in viewing structures. Like **10**, structures **8** and **9** are representative of known synthetic species: cuboidal clusters $[Fe_4S_3(NO)_7]^{1-}$ [80,81] and $Fe_4S_3(NO)_4(PPh_3)_3$ [46], and prismane clusters $[Fe_6S_6Cl_6]^{2-,3-}$ [60,82].

Some iron–sulfur clusters, including many of those found in proteins (**2–6**), do not derive *directly* from the antifluorite parent structure. Clusters of this type are, however, readily obtained from antifluorite fragments by performing one (or more) of four simple cluster rearrangements. Many of the clusters generated from antifluorite fragments contain proximal tetrahedral edges, which, provided the structure exhibits the required flexibility, may be merged to form a new cluster. The procedure is demonstrated by way of example in Fig. 4. Here cuboidal 'fragment' cluster **8** is manipulated

Table 2
Enumeration [a] of database (D) clusters $Fe_mS_qL_l$

m	Origin			Total	u.l. + μ_{2-4} [d]
	Fragments [b]	Folding	Other [c]		
2	1			1	
3	2	1		3	1
4	9	4		13	2
5	29	26	2	57	6
6	165	177		342	16
7	962	1153	9	2124	72
8	6423	6755	7	13185	257

[a] Numbers represent upper bounds for $m = 7, 8$; for chiral clusters, only one enantiomer is counted.

[b] Clusters directly derived from pieces of the Fe_2S parent solid.

[c] Clusters arising from closure, fusion or condensation processes and not obtained as fragments or by way of folding.

[d] Uniterminally ligated with S bridging modalities restricted to μ_{2-4}.

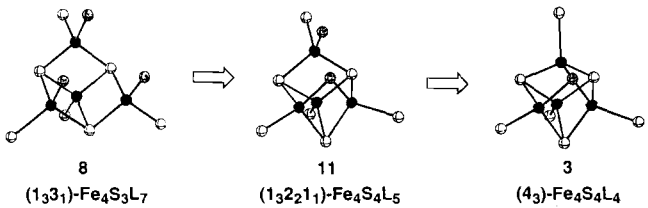

Fig. 4. Formation of cubane structure **3** from cuboidal structure **8** by two successive folding operations. The lower portion of cluster **8** is folded across such that the lower two shaded L atoms coalesce (as do the corresponding tetrahedral edges) into a single S atom to yield a new cluster, **11**. The lower portion of **11** (equivalent to **2**) is rigid, however, the upper tetrahedron may be folded down, coalescing two shaded atoms (one S and one L) to form cubane cluster **3**.

once to form **11**, and again to yield the cubane cluster **3**. This process is called *folding*, and the importance of its contribution to our iron–sulfur cluster family is evident from the large number of new structures it produces (see Table 2). Other types of rearrangement processes make far smaller contributions to the database, and may be dealt with briefly. The closure operation involves excising pieces from an infinite one- (chain cyclization) or two- (sheet wrapping) dimensional edge-sharing tetrahedra-based structure. These pieces are then flexed or wrapped around such that the newly exposed edges join to form finite clusters which are topologically equivalent to the original infinite structure. Processes in which two separate clusters are merged by superposing atoms or forging new intercluster bonds are called fusion and condensation, respectively. Cluster **5**, for example, may be attained from two cubane units (**3**), by fusion via two cysteinates coupled with condensation to form an S–S bond. All appropriate new structures arising from cluster rearrangement processes are added to the iron–sulfur database; these are enumerated in Table 2.

As set out in Table 2, the total number of database clusters increases rapidly with the number of iron centers, m. It is, therefore, helpful to apply certain criteria that sort clusters of particular interest from the database. Two such restrictive criteria which have been recognized through simple empirical observations are present in the forms of uniterminal ligation and S atom bridging modalities [76]. A cluster is uniterminally ligated if each iron atom is coordinated by one or fewer terminal ligands L. For example, **3** is uniterminally ligated, while **8** is not due to the three iron atoms each with two terminal ligands. *All structurally proven iron–sulfur clusters with more than four iron atoms exhibit uniterminal ligation. Similarly, bridging modalities of the sulfur atoms are limited to μ_2, μ_3 or μ_4 in all proven iron–sulfur clusters.* Table 2 conveys the efficacy of these restrictions in reducing the number of structures worthy of detailed examination.

3. The protein-bound subset

A subset of potential protein-bound clusters is readily extracted from the iron–sulfur cluster database (D). Any database cluster with an Fe:S ratio near unity shall be considered a member of the subset:

$$\{Fe_mS_{m-1}L_l,\ Fe_mS_mL_l,\ Fe_mS_{m+1}L_l\} \subset D$$

This condition is based on the observed iron–sulfur core stoichiometries in structurally resolved (**1–6**) biomolecules. The elements of the subset are considered likely canditates for protein-bound clusters, and merit further examination. If desired, the treatment can be extended to Fe:S ratios of larger range, but that will not be done here.

3.1. Bi-, tri- and tetranuclear clusters

Subset clusters of nuclearity four or less are enumerated by formula in Table 3. Since uniterminal ligation does not necessarily hold for these nuclearities, all of the clusters must be considered a priori as equally likely to arise in proteins. Their structures are illustrated in Fig. 5. Cluster **1**, already demonstrated in protein-bound form [2–10], represents the single binuclear possibility. Two of the three trinuclear clusters exhibit Fe_3S_4 cores with known structures: **2** is present in numerous proteins [11–18] and **7** may be prepared synthetically [42]. The other cluster, **12**, contains an unprecedented Fe_3S_3 core. No potential clusters with Fe_3S_2 cores are obtained. Of the twelve different tetranuclear clusters, only the cubane **3** has been observed in proteins [14–31]. Representing the sole $Fe_4S_3L_l$ candidate, cuboidal structure **8** is found in two synthetic forms [46,80,81], as described above. The μ_2-S atom

Table 3
Enumeration of potential protein-bound clusters: $Fe_{2-4}S_qL_l$ ($q = m-1$, m, $m+1$)

Formula	Total	Fragments[a]	u.l.[b]	Structures[c]
$Fe_2S_2L_4$	1	1		**1**
$m=2$	1	1		
$Fe_3S_3L_5$	1	1		**12**
$Fe_3S_4L_3$	1		1	**2**
$Fe_3S_4L_4$	1	1		**7**
$m=3$	3	2	1	
$Fe_4S_3L_7$	1	1		**8**
$Fe_4S_4L_4$	1		1	**3**
$Fe_4S_4L_5$	1			**11**
$Fe_4S_4L_6$	5	5		**13–17**
$Fe_4S_5L_4$	3	1	1	**18–20**
$Fe_4S_5L_5$	1	1		**21**
$m=4$	12	8	2	

[a] Clusters directly derived from edge-sharing antifluorite fragments.
[b] Uniterminally ligated.
[c] See Fig. 5.

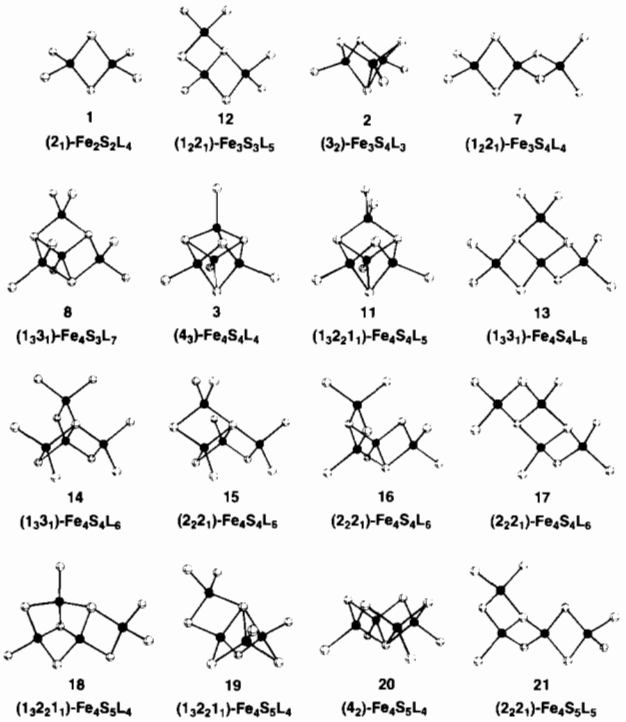

Fig. 5. Low nuclearity ($m \leq 4$) candidates for protein-bound iron–sulfur clusters. Clusters **2**, **3**, **11**, **18** and **19** contain folds, while the other clusters derive directly from antifluorite fragments. Only **2**, **3** and **20** are uniterminally ligated.

and the top foremost L atom (i.e., the two gray atoms in the Fig. 4 depiction) of cluster **11**, are in rather close contact (2.1 Å) as drawn. This S–L steric interaction may be alleviated by flexing the uppermost FeX_4 (X = S, L) tetrahedron in a direction opposite to that used to make the final fold in Fig. 4. Alternatively, the ligand L may be formulated as an S atom, forging an S–S bond to yield a new cluster $Fe_4S_5L_4$ (**22**). The core geometry of **22** is present in dimeric form in the synthetic cluster $Fe_8S_{12}(CN^tBu)_{12}$ [83]. The remaining nine clusters are unknown in iron–sulfur chemistry. However, structural precedence for **13** and **20** is found in the clusters $[MCu_3S_4(S_2CNEt_2)_3]^{2-}$ (M = Mo, W) [84,85] and $[Cu_4(ettu)_9]^{4+}$ (ettu = ethylenethiourea) [86], respectively, when all bridging sulfur atoms are treated as sulfide.

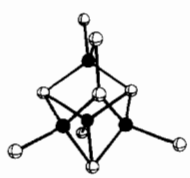

22

3.2. $Fe_5S_{4-6}L_l$

There are fifty pentanuclear subset clusters with seven different possible stoichiometries, as enumerated in Table 4. Of these, five (**26–30** in Fig. 6) meet the uniterminal ligation and S atom bridging modality criteria, and consequently represent the most likely candidates for protein-bound clusters. One (**26**) contains an Fe_5S_5 core, while four (**27–30**) display Fe_5S_6 cores. Serving as the only relevant pentanuclear examples in iron–sulfur chemistry, synthetic $MFe_4S_6(PEt_3)_4Cl$ (M = V, Mo) clusters [47,48] adopt a structure congruent with **29** in which the heterometal occupies the non-edge-sharing (1_0) position. The other four (indeed, the other forty-nine) structures are without precedent.

When testing models for protein-bound clusters, it may sometimes be prudent (or necessary) to consider structures which fail to meet our selection criteria. This is particularly true in view of the ability of the protein environment to stabilize unprecedented structures. Thus, in selecting certain clusters (such as **26–30** above) our intention is merely to isolate the most likely protein-

Table 4
Enumeration of potential protein-bound clusters: $Fe_5S_{4-6}L_l$

Formula	Total	Fragments [a]	u.l. + μ_{2-4} [b]	Structures [c]
$Fe_5S_4L_8$	3	3		**23–25**
$Fe_5S_5L_5$	2		1	**26**
$Fe_5S_5L_6$	7	1		
$Fe_5S_5L_7$	11	11		
$Fe_5S_6L_4$	2		2	**27, 28**
$Fe_5S_6L_5$	16	2	2	**29, 30**
$Fe_5S_6L_6$	9	9		
$m = 5$	50	26	5	

[a] Clusters directly derived from edge-sharing antifluorite fragments.
[b] Uniterminally ligated with S bridging modalities restricted to μ_{2-4}.
[c] See Fig. 6.

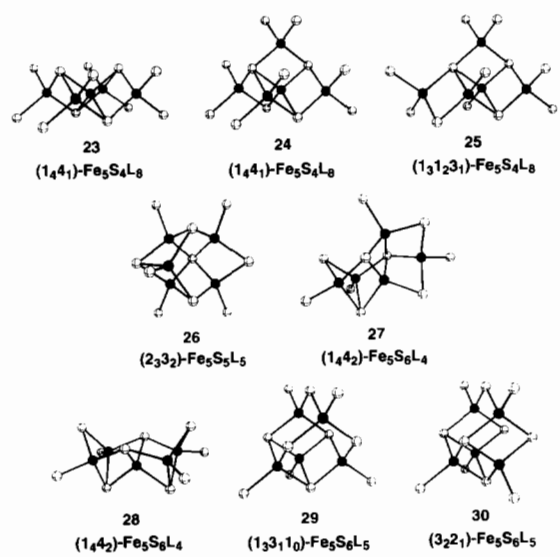

Fig. 6. Candidates for protein-bound clusters containing Fe_5S_{4-6} cores. Clusters **23–25**, **29** and **30** are all directly derived from fragments of the antifluorite structure (compare with Fig. 2). Clusters **26–30** meet the selection criteria; **23–25** are not uniterminally ligated.

bound candidates, which should therefore be assayed first. If the selected structures do not fit the observed electron density, or if no suitable clusters meet the selection criteria, then the remaining possibilities should be examined. For example, suppose experimental evidence indicated the presence of an Fe_5S_4 core in a protein under crystallographic investigation. Inspection of Table 4 reveals that none of the subset clusters which fulfill our selection conditions have this core composition. Examining the other possibilities, however, unveils three $Fe_5S_4L_8$ clusters, which, given their formulae, cannot be uniterminally ligated. These clusters, shown at the top of Fig. 6 (**23–25**), provide three stereochemically reasonable models for testing, and should not be overlooked despite the lack of precedence for a pentanuclear iron–sulfur cluster without uniterminal ligation.

3.3. $Fe_6S_{5-7}L_l$

Spanning twelve different stoichiometries, the 280 hexanuclear subset clusters are enumerated in Table 5. The ten which meet our selection requirements (Fig. 7) include one Fe_6S_5 (**31**), four Fe_6S_6 (**9**, **32–34**) and five Fe_6S_7 (**35–39**) core-containing clusters. Synthetic clusters with the basket structure (**34**) have been prepared in the forms $Fe_6S_6(PR_3)_4L_2$ ($L=RS^-$, Cl^-, Br^-) [87–89] and $[Fe_6S_6(PEt_3)_6]^{1+}$ [90]. As mentioned earlier, synthetic prismane clusters (**9**) such as $[Fe_6S_6Cl_6]^{2-}$ [82] and $[Fe_6S_6L_6]^{3-}$ ($L=RS^-$, Cl^-) [59,60] are also known. Of the other eight structures, only **31**, which is adopted by $Ni_6Se_5(PPh_3)_6$ [91], has any precedence. Structures **9**, **33** and **34** are closely related, and may be derived by extracting two FeL moieties from **10** in all of the three different possible ways. Clusters **38** and **39** each contain one short intersulfur contact, generating a prospective S–S bonding interaction. This would have little effect on the rest of their respective structures, and no effect on their stoichiometries.

Table 5
Enumeration of potential protein-bound clusters: $Fe_6S_{5-7}L_l$

Formula	Total	Fragments [a]	u.l. + μ_{2-4} [b]	Structures [c]
$Fe_6S_5L_6$	2		1	**31**
$Fe_6S_5L_7$	1			
$Fe_6S_5L_8$	5			
$Fe_6S_5L_9$	11	11		
$Fe_6S_6L_5$	1		1	**32**
$Fe_6S_6L_6$	19	3	3	**9**, **33**, **34**
$Fe_6S_6L_7$	51	10		
$Fe_6S_6L_8$	51	51		
$Fe_6S_7L_4$	3		1	**35**
$Fe_6S_7L_5$	27		4	**36–39**
$Fe_6S_7L_6$	68	22		
$Fe_6S_7L_7$	41	41		
$m=6$	280	138	10	

[a] Clusters directly derived from edge-sharing antifluorite fragments.
[b] Uniterminally ligated with S bridging modalities restricted to μ_{2-4}.
[c] See Fig. 7.

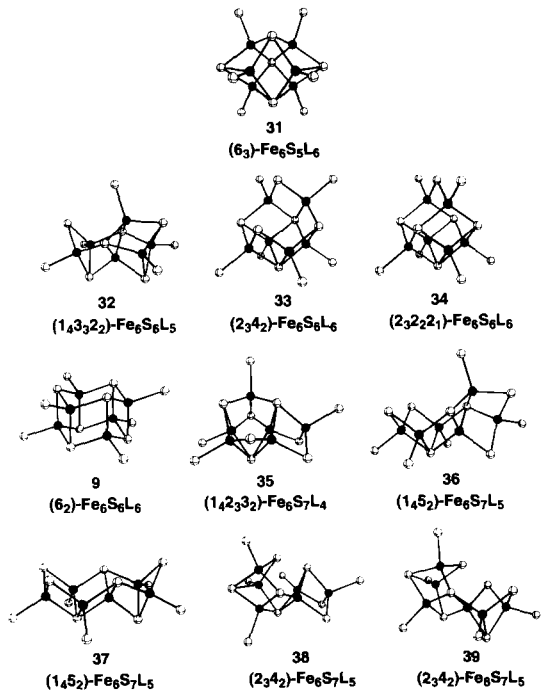

Fig. 7. All uniterminally ligated, hexanuclear members of the protein-bound subset containing strictly μ_{2-4}-S atom bridges. Only **9**, **33** and **34**, derive directly from antifluorite fragments; the rest contain folds.

Structures **9** and **31–39** are all worthy candidates for the six-iron clusters detected in *Desulfovibrio vulgaris* (Hildenborough) [57,58] and *Desulfovibrio desulfuricans* [61]. Given the experimental evidence [59–61], **9** is the obvious choice as an initial model in both cases. Barring its immediate success, some or all of **31–39** might follow in whatever order deemed appropriate. The failure of any of these models to account for the observed electron density would, of course, warrant examination of the remaining clusters listed in Table 5.

3.4. $Fe_7S_{6-8}L_l$

The protein-bound subset contains well over a thousand heptanuclear clusters, which are enumerated by their fifteen possible chemical formulae in Table 6. Forty-one of these meet the selection criteria. The only one with an Fe_7S_6 core is (4_33_2)-$Fe_7S_6L_7$ (see **40**), which is readily derived from **10** by removing a single FeL moiety. A synthetic example of cluster **40** is provided by $Fe_7S_6(PEt_3)_4Cl_3$ [92]. Thirteen selected clusters have Fe_7S_7 cores with either six or seven (**47–53**) attendant ligands, L. The six $Fe_7S_7L_6$ clusters (**41–46**, Fig. 8) exhibit rather unsymmetrical structures, with C_s (**41**, **46**) being the only point group symmetry greater than C_1 (**42–45**). The seven somewhat more appealing $Fe_7S_7L_7$ structures (**47–53**) are shown in Fig. 9. Fusion of **2** and **8** produces **51**, which is the exact structure adopted

Table 6
Enumeration [a] of potential protein-bound clusters: $Fe_7S_{6-8}L_l$

Formula	Total	Fragments [b]	u.l. + μ_{2-4} [c]	Structures [d]
$Fe_7S_6L_6$	1			
$Fe_7S_6L_7$	8	1	1	**40**
$Fe_7S_6L_8$	19			
$Fe_7S_6L_9$	69	9		
$Fe_7S_6L_{10}$	62	62		
$Fe_7S_7L_5$	3			
$Fe_7S_7L_6$	34		6	**41–46**
$Fe_7S_7L_7$	163	13	7	**47–53**
$Fe_7S_7L_8$	266	78		
$Fe_7S_7L_9$	213	213		
$Fe_7S_8L_4$	4		2	
$Fe_7S_8L_5$	68		8	
$Fe_7S_8L_6$	207	8	17	
$Fe_7S_8L_7$	304	137		
$Fe_7S_8L_8$	250	250		
$m=7$	1671	771	41	

[a] Numbers represent upper bounds for formulae with $(q+l)<2m$.
[b] Clusters directly derived from edge-sharing antifluorite fragments.
[c] Uniterminally ligated with S bridging modalities restricted to μ_{2-4}.
[d] See Figs. 8 and 9.

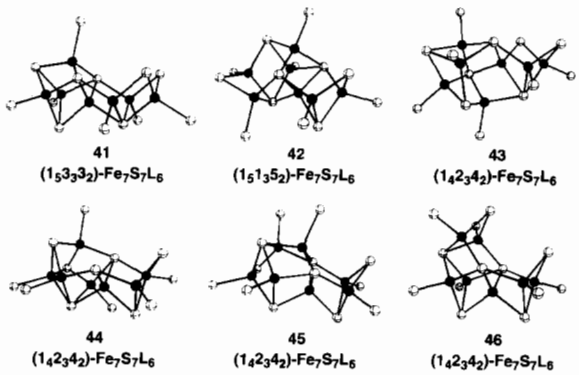

Fig. 8. The six isomeric $Fe_7S_7L_6$ subset clusters which meet the uniterminal ligation and bridging modality criteria. All contain folds.

by $Ga_7S_7(^tBu)_7$ [93]. The closely related structures of **48–50**, **52** and **53** are all derived by extracting three capping FeL units from decanuclear (10_3)-$Fe_{10}S_7L_{10}$ (see **54**), a highly symmetrical (D_{5h}) cluster in which the S atoms form a pentagonal bipyramid with each face capped radially by an FeL unit. Twenty-seven selected clusters contain Fe_7S_8 cores bound by four, five or six terminal ligands; their structures are too numerous to show.

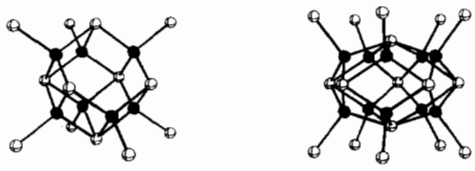

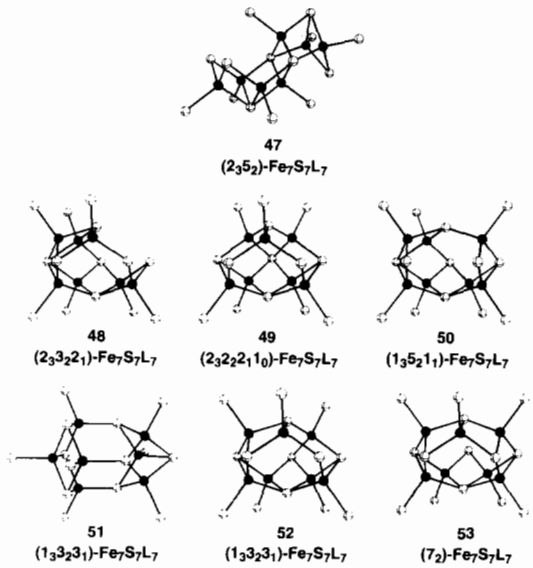

Fig. 9. The seven isomeric $Fe_7S_7L_7$ subset clusters which meet the selection criteria.

Table 7
Enumeration [a] of potential protein-bound clusters: $Fe_8S_{7-9}L_l$

Formula	Total	Fragments [b]	u.l. + μ_{2-4} [c]	Structures
$Fe_8S_7L_6$	1			
$Fe_8S_7L_7$	14			
$Fe_8S_7L_8$	93	5	3	
$Fe_8S_7L_9$	222	13		
$Fe_8S_7L_{10}$	440	95		
$Fe_8S_7L_{11}$	319	319		
$Fe_8S_8L_5$	4			
$Fe_8S_8L_6$	79		1	
$Fe_8S_8L_7$	386		18	
$Fe_8S_8L_8$	1028	146	3	
$Fe_8S_8L_9$	1267	553		
$Fe_8S_8L_{10}$	1127	1127		
$Fe_8S_9L_4$	6			**57**
$Fe_8S_9L_5$	137		19	
$Fe_8S_9L_6$	631	8	41	
$Fe_8S_9L_7$	1218	116	24	
$Fe_8S_9L_8$	1526	957	1	**55**
$Fe_8S_9L_9$	1390	1390		
$m=8$	9888	4729	110	

[a] Numbers represent upper bounds for formulae with $(q+l)<2m$.
[b] Clusters directly derived from edge-sharing antifluorite fragments.
[c] Uniterminally ligated with S bridging modalities restricted to μ_{2-4}.

3.5. $Fe_8S_{7-9}L_l$

Nearly ten thousand clusters comprise the octanuclear members of the protein-bound subset. They range across eighteen possible stoichiometries, as enumerated in Table 7. Of the 110 which meet our selection criteria, 3, 22 and 85 contain Fe_8S_7, Fe_8S_8 and Fe_8S_9 cores, respectively. Again, there are too many structures to present here. We shall, however, focus on two nitrogenase-related clusters.

The first represents an all-iron, all-tetrahedral version of the nitrogenase cofactor (**6**). This $Fe_8S_9L_8$ cluster (**55**) is obtained through fusion of two cuboidal clusters with structure **8**, and is depicted at the top of Fig. 10. Although **55** and **6** display the same core connectivity, there are clearly important geometrical differences which must be reconciled. The linear stereochemistry of the μ_2-S atoms in **55** may be altered by flexing the entire cluster about its waist, producing a more reasonable bent sulfur coordination, as shown in the middle of Fig. 10. As demonstrated here, any flexibility associated with a particular structure must be fully explored before it can be rejected as a model. Imposing an inward trigonal distortion on the six central iron atoms now draws the two 'cuboidal' halves into more intimate contact, resulting in cluster **56** with a core geometry matching that of the cofactor **6**. Such a trigonal distortion is not uncommon in iron–sulfur clusters at iron atoms bound by terminal phosphines (L = phosphine) [47,48,87–90], and the perturbation involved should generally be small enough to readily arise during refinement of the original undistorted structure. Thus, a cluster $Fe_8S_9(PR_3)_6L_2$ with structure **56**, would certainly appear to be a reasonable synthetic target as a stable structural model for the nitrogenase cofactor.

The second nitrogenase-related cluster (two views are shown in **57**) has the formula (4_44_3)-$Fe_8S_9L_4$, with a core geometry corresponding to that of the most recent P-cluster structure [35]. As mentioned previously, this geometry is related to that of **5** through formal replacement of S_2^{2-} by S^{2-}. Cluster **57** is uniterminally ligated, but the μ_6-S atom clearly violates our μ_{2-4} selection criterion. Significantly, none of the other five $Fe_8S_9L_4$ clusters listed in Table 7 conform to this criterion either. While six-fold sulfur coordination is unprecedented in iron–sulfur cluster chemistry, it has been demonstrated in trigonal prismatic form for the cluster $[Ni_8S(S^tBu)_9]^-$ [94]. It is reasonable to expect that as cluster nuclearity increases, so will the likelihood of encountering higher-coordinate sulfur atoms. Thus, in considering structures with $m \geqslant 8$, some care should be taken not to over-emphasize the importance of sulfur atom bridging modality.

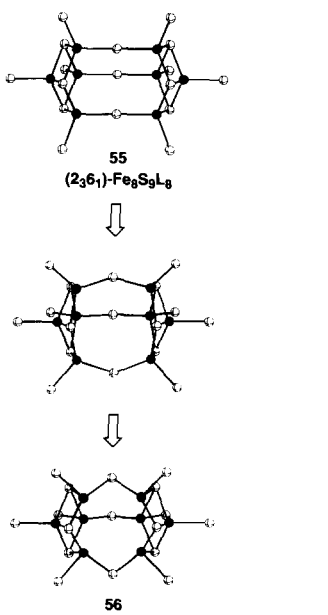

Fig. 10. Transformation of **55** into **56**, a cluster closely related to the nitrogenase cofactor (**6**). The top two structures contain only ideal iron-centered tetrahedra, while the coordination of the size equivalent iron atoms in **56** is trigonal pyramidal, with an L–Fe–S angle of 90°.

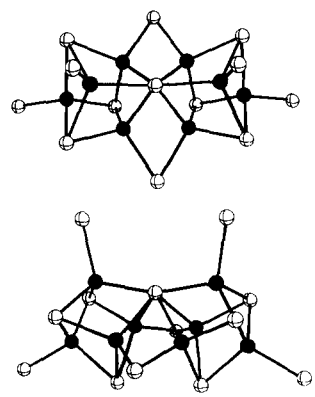

57

4. Laser ablated cluster ions

Recent work has shown that laser ablation of iron- and sulfur-containing solids generates a series of cluster ions with compositions $[Fe_mS_{m-1}]^-$, $[Fe_mS_m]^-$ and $[Fe_mS_{m+1}]^-$ [95]. These are, of course, precisely the core compositions selected for our protein-bound subset. Photodissociation studies performed on similarly obtained cluster ions indicate a possible relationship between their structures and the core topologies displayed in synthetic and protein-bound iron–sulfur clusters [96]. If this relationship holds, then stripping the terminal ligands, L, off our subset clusters should provide an exhaustive source of potential cluster ion structures. These structures are enumerated in Table 8. Very likely those cluster ions which derive from uniterminally ligated cluster cores will be more stable, since three- or four-coordinate iron atoms should be favored over two-coordinate iron atoms. Thus, the previously employed selection criteria should still be effective. Nevertheless, it seems probable that the structures would undergo some relaxation in the absence of saturating terminal ligands. Given an appropriate set of iron and sulfur parameters, it should be possible to simulate this relaxation through molecular mechanics.

Table 8
Enumeration [a] of potential laser-ablated cluster ions

Formula	Total	Fragments [b]	u.l. + μ_{2-4} [c]	Structures [d]
$[Fe_2S_2]^-$	1	1		**1**
$[Fe_3S_3]^-$	1	1		**12**
$[Fe_3S_4]^-$	2	1	1	**2, 7**
$[Fe_4S_3]^-$	1	1		**8**
$[Fe_4S_4]^-$	7	5	1	**3, 11, 13–17**
$[Fe_4S_5]^-$	4	2	1	**18–21**
$[Fe_5S_4]^-$	3	3		**23–25**
$[Fe_5S_5]^-$	20	12	1	**26**
$[Fe_5S_6]^-$	27	11	4	**27–30**
$[Fe_6S_5]^-$	19	11	1	**31**
$[Fe_6S_6]^-$	122	64	4	**9, 32–34**
$[Fe_6S_7]^-$	139	63	5	**35–39**
$[Fe_7S_6]^-$	159	72	1	**40**
$[Fe_7S_7]^-$	679	304	13	**41–53**
$[Fe_7S_8]^-$	833	395	27	
$[Fe_8S_7]^-$	1089	463	3	
$[Fe_8S_8]^-$	3891	1826	22	
$[Fe_8S_9]^-$	4908	2471	85	**55, 57**

[a] Numbers represent upper bounds for $m = 7$, 8.
[b] Cluster ions directly derived from antifluorite fragments.
[c] Cluster ions derived from the cores of uniterminally ligated clusters with S bridging modalities restricted to μ_{2-4}.
[d] Core of referenced cluster depiction.

5. Conclusions

A computer-generated database has been employed in exploring potential new structures for protein-bound iron–sulfur clusters. Containing an exhaustive collection of edge-sharing tetrahedra-based $Fe_mS_qL_l$ clusters, the database was created by extricating fragments from a parent solid with the antifluorite structure, and, whenever appropriate, subjecting them to various structural rearrangements [75]. On the basis of observed biological stoichiometries, a protein-bound subset consisting of all clusters with formulae $Fe_mS_{m-1}L_l$, $Fe_mS_mL_l$ and $Fe_mS_{m+1}L_l$ is extracted from the database. The clusters are enumerated by formula for nuclearities, m, of eight or less (Tables 3–7). Subset members which meet specific ligation (uniterminal) and bridging modality (μ_{2-4}-S) criteria are considered likely candidates for protein-bound clusters, and many of their structures are examined in detail (Figs. 5–9). Ideally, the structures supplied herein would serve as models during crystal structure determination of proteins containing novel iron–sulfur clusters. If required, the treatment is readily expanded to include a broader range of Fe_mS_q core compositions (as well as higher nuclearities, m), and these structures may be sorted in a manner analogous to that described above. An additional application of the subset involves elucidation of laser ablated cluster ions; possible structures are enumerated for $[Fe_mS_{m-1}]^-$, $[Fe_mS_m]^-$ and $[Fe_mS_{m+1}]^-$ ($m \leq 8$) in Table 8.

6. Supplementary material

Tables of coordinates for cluster structures **1–57** are available upon request from author R.H.H.

Acknowledgements

This work was funded by NIH Grant GM 28856. We thank the Office of Naval Research for its support of J.R.L. in the form of a predoctoral fellowship (1991–1994), and Professor J.T. Bolin for supplying his coordinates for the nitrogenase P-cluster.

References

[1] R. Cammack (ed.), *Advances in Inorganic Chemistry,* Vol. 38, Academic Pres, New York, 1992.
[2] T. Tsukihara, K. Fukuyama, H. Tahara, Y. Katsube, Y. Matsuura, N. Tanaka, M. Kakudo, K. Wada and H. Matsubara, *J. Biochem. (Tokyo), 84* (1978) 1645.
[3] K. Fukuyama, T. Hase, S. Matsumoto, T. Tsukihara, Y. Katsube, N. Tanaka, M. Kakudo, K. Wada and H. Matsubara, *Nature, 286* (1980) 522.
[4] T. Tsukihara, K. Fukuyama, M. Nakamura, Y. Katsube, N. Tanaka, M. Kakudo, K. Wada, T. Hase and H. Matsubara, *J. Biochem. (Tokyo), 90* (1981) 1763.
[5] T. Tsukihara, K. Fukuyama, M. Mizushima, T. Harioka, M. Kusunoki, Y. Katsube, T. Hase and H. Matsubara, *J. Mol. Biol., 216* (1990) 399.
[6] J.L. Sussman, J.H. Brown and M. Shoham, in H. Matsubara, Y. Katsube and K. Wada (eds.), *Iron–Sulfur Protein Research,* Springer, New York, 1987, pp. 69–81.
[7] J.L. Sussman, M. Shoham and M. Harel, *Prog. Clin. Biol. Res., 289* (1989) 171.
[8] W.R. Rypniewski, D.R. Breiter, M.M. Benning, G. Wesenberg, B.-H. Oh, J.L. Markley, I. Rayment and H.M. Holden, *Biochemistry, 30* (1991) 4126.
[9] H.M. Holden, B.L. Jacobson, J.K. Hurley, G. Tollin, B.-H. Oh, L. Skjeldal, Y.K. Chae, H. Cheng, B. Xia and J.L. Markley, *J. Bioenerg. Biomemb., 26* (1994) 67.
[10] B.L. Jacobson, Y.K. Chae, J.L. Markley, I. Rayment and H.M. Holden, *Biochemistry, 32* (1993) 6788.
[11] A.H. Robbins and C.D. Stout, *Proteins, 5* (1989) 289.
[12] C.R. Kissinger, E.T. Adman, L.C. Sieker and L.H. Jensen, *J. Am. Chem. Soc., 110* (1988) 8721.
[13] C.R. Kissinger, L.C. Sieker, E.T. Adman and L.H. Jensen, *J. Mol. Biol., 219* (1991) 693.
[14] G.H. Stout, S. Turley, L.C. Sieker and L.H. Jensen, *Proc. Natl. Acad. Sci. U.S.A., 85* (1988) 1020.
[15] C.D. Stout, *J. Biol. Chem., 263* (1988) 9256.
[16] C.D. Stout, *J. Mol. Biol., 205* (1989) 545.
[17] A.E. Martin, B.K. Burgess, C.D. Stout, V.L. Cash, D.R. Dean, G.M. Jensen and P.J. Stephens, *Proc. Natl. Acad. Sci., U.S.A., 87* (1990) 598.
[18] J. Soman, S. Iismaa and C.D. Stout, *J. Biol. Chem., 266* (1991) 21558.
[19] C.W. Carter, Jr., J. Kraut, S.T. Freer, N.-H. Xuong, R.A. Alden and R.G. Bartsch, *J. Biol. Chem., 249* (1974) 4212.
[20] C.W. Carter, Jr., J. Kraut, S.T. Freer and R.A. Alden, *J. Biol. Chem., 249* (1974) 6339.
[21] S.T. Freer, R.A. Alden, C.W. Carter, Jr. and J. Kraut, *J. Biol. Chem., 250* (1975) 49.

[22] K. Fukuyama, H. Matsubara, T. Tsukihara and Y. Katsube, *J. Mol. Biol., 210* (1989) 383.
[23] C.-F. Kuo, D.E. McRee, C.L. Fisher, S.F. O'Handley, R.P. Cunningham and J.A. Tainer, *Science, 258* (1992) 434.
[24] D.R. Breiter, T.E. Meyer, 1. Rayment and H.M. Holden, *J. Biol. Chem., 266* (1991) 18660.
[25] L.W. Lim, N. Shamala, F.S. Mathews, D.J. Steenkamp, R. Hamlin and N.H. Xuong, *J. Biol. Chem., 261* (1986) 15140.
[26] I. Rayment, G. Wesenberg, T.E. Meyer, M.A. Cusanovich and H.M. Holden, *J. Mol. Biol., 228* (1992) 672.
[27] E.T. Adman, L.C. Sieker and L.H. Jensen, *J. Biol. Chem., 248* (1973) 3987; *251* (1976) 3801.
[28] G. Backes, Y. Mino, T.M. Loehr, T.E. Meyer, M.A. Cusanovich, W.V. Sweeney, E.T. Adman and J. Sanders-Loehr, *J. Am. Chem. Soc., 113* (1991) 2055.
[29] M.M. Benning, T.E. Meyer, I. Rayment and H.M. Holden, *Biochemistry, 33* (1994) 2476.
[30] A.H. Robbins and C.D. Stout, *Proc. Natl. Acad. Sci. U.S.A., 86* (1989) 3639.
[31] M.M. Georgiadis, H. Komiya, P. Chakrabarti, D. Woo, J.J. Kornuc and D.C. Rees, *Science, 257* (1992) 1653.
[32] J. Kim and D.C. Rees, *Nature, 360* (1992) 553.
[33] M.K. Chan, J. Kim and D.C. Rees, *Science, 260* (1993) 792.
[34] J. Kim, D. Woo and D.C. Rees, *Biochemistry, 32* (1993) 7104.
[35] J.T. Bolin, personal communication.
[36] B.K. Burgess, *Chem. Rev., 90* (1990) 1377.
[37] J. Kim and D.C. Rees, *Biochemistry, 33* (1994) 389.
[38] J.M. Berg and R.H. Holm, in T.G. Spiro (ed.), *Iron–Sulfur Proteins,* Wiley-Interscience, New York, 1982, Ch. 1, and refs. therein.
[39] P.A. Lindahl and J.A. Kovacs, *J. Cluster Sci., 1* (1990) 29.
[40] T.D.P. Stack, J.A. Weigel and R.H. Holm, *Inorg. Chem., 29* (1990) 3745.
[41] R.H. Holm, S. Ciurli and J.A. Weigel, *Prog. Inorg. Chem., 38* (1990) 1.
[42] K.S. Hagen, A.D. Watson and R.H. Holm, *J. Am. Chem. Soc., 105* (1983) 3905.
[43] M.C. Kennedy, T.A. Kent, M. Emptage, H. Merkle, H. Beinert and E. Münck, *J. Biol. Chem., 259* (1984) 14463.
[44] H.-Y. Zhuang and A.G. Sykes, *J. Chem. Soc., Dalton Trans.,* (1994) 1025.
[45] R.H. Holm, *Adv. Inorg. Chem., 38* (1992) 1.
[46] M.J. Scott and R.H. Holm, *Angew. Chem., Int. Ed. Engl., 32* (1993) 564.
[47] E. Nordlander, S.C. Lee, W. Cen, Z.Y. Wu, C.R. Natoli, A. Di Cicco, A. Filipponi, B. Hedman, K.O. Hodgson and R.H. Holm, *J. Am. Chem. Soc., 115* (1993) 5549.
[48] W. Cen, F.M. MacDonnell, M.J. Scott and R.H. Holm, *Inorg. Chem., 33* (1994) in press.
[49] R.H. Holm and E.D. Simhon, in T.G. Spiro (ed.), *Molybdenum Enzymes,* Wiley-Interscience, New York, 1985, Ch. 1.
[50] D. Coucouvanis, *Acc. Chem. Res., 24* (1991) 1.
[51] J. Zhou, M.J. Scott, Z. Hu, G. Peng, E. Münck and R.H. Holm, *J. Am. Chem. Soc., 114* (1992) 10843.
[52] M.W.W. Adams, *Biochim. Biophys. Acta, 1020* (1990) 115.
[53] H. Thomann, M. Bernardo and M.W.W. Adams, *J. Am. Chem. Soc., 113* (1991) 7044.
[54] A.J. Pierik, W.R. Hagen, J.S. Redeker, R.B.G. Wolbert, M. Boersma, M.F.J.M. Verhagen, H.J. Grande, C. Veeger, P.H.A. Mutsaers, R.H. Sands and W.R. Dunham, *Eur. J. Biochem., 209* (1992) 63.
[55] C. Hatchikian, N. Forget, V.M. Fernandez, R. Williams and R. Cammack, *Eur. J. Biochem., 209* (1992) 357.
[56] W. Fu, P.M. Drozdzewski, T.V. Morgan, L.E. Mortenson, A. Juszczak, M.W.W. Adams, S.-H. He, H.D. Peck, Jr., D.V. DerVartanian, J. LeGall and M.K. Johnson, *Biochemistry, 32* (1993) 4813.
[57] W.R. Hagen, A.J. Pierik and C. Veeger, *J. Chem. Soc., Faraday Trans. 1* (1989) 4083.
[58] J.P.W.G. Stokkermans, A.J. Pierik, R.B.G. Wolbert, W.R. Hagen, W.M.A.M. Van Dongen and C. Veeger, *Eur. J. Biochem., 208* (1992) 435.
[59] M.G. Kanatzidis, W.R. Hagen, W.R. Dunham, R.K. Lester and D. Coucouvanis, *J. Am. Chem. Soc., 107* (1985) 953.
[60] M.G. Kanatzidis, A. Salifoglou and D. Coucouvanis, *Inorg. Chem., 25* (1986) 2460.
[61] I. Moura, P. Tavares, J.J.G. Moura, N. Ravi, B.H. Huynh, M.-Y. Liu and J. LeGall, *J. Biol. Chem., 267* (1992) 4489.
[62] A.J. Pierik and W.R. Hagen, *Eur. J. Biochem., 195* (1991) 505.
[63] M.S.M. Jetten, A.J. Pierik and W.R. Hagen, *Eur. J. Biochem., 202* (1991) 1291.
[64] A. Müller and E. Diemann, *Adv. Inorg. Chem., 31* (1987) 89.
[65] D. Fenske, J. Ohmer, J. Hachgenei and K. Nerzweiler, *Angew. Chem., Int. Ed. Engl., 27* (1988) 1277.
[66] P. Zanello, *Coord. Chem. Rev., 83* (1988) 199.
[67] S. Harris, *Polyhedron, 8* (1989) 2843.
[68] S.C. Lee and R.H. Holm, *Angew. Chem., Int. Ed. Engl., 29* (1990) 840.
[69] M.A. Ansari and J.A. Ibers, *Coord. Chem. Rev., 100* (1990) 223.
[70] B. Krebs and G. Henkel, *Angew. Chem., Int. Ed. Engl., 30* (1991) 769.
[71] T. Shibahara, *Adv. Inorg. Chem., 37* (1991) 143.
[72] T. Shibahara, *Coord. Chem. Rev., 123* (1993) 73.
[73] L.C. Roof and J.W. Kolis, *Chem. Rev., 93* (1993) 1037.
[74] I. Dance and K. Fisher, *Prog. Inorg. Chem., 41* (1994) 637.
[75] J.R. Long and R.H. Holm, *J. Am. Chem. Soc., 116* (1994) in press.
[76] J.-F. You and R.H. Holm, *Inorg. Chem., 31* (1992) 2166.
[77] S. Pohl and W. Saak, *Angew. Chem., Int. Ed. Engl., 23* (1984) 907.
[78] W. Saak and S. Pohl, *Angew. Chem., Int. Ed. Engl., 30* (1991) 881.
[79] S. Pohl and U. Optiz, *Angew. Chem., Int. Ed. Engl., 32* (1993) 863.
[80] C.T.-W. Chu and L.F. Dahl, *Inorg. Chem., 16* (1977) 3245.
[81] C. Glidewell, R.J. Lambert, M.E. Harman and M.B. Hursthouse, *J. Chem. Soc., Dalton Trans.,* (1990) 2685.
[82] D. Coucouvanis, M.G. Kanatzidis, W.R. Dunham and W.R. Hagen, *J. Am. Chem. Soc., 106* (1984) 7998.
[83] L. Cai, M.J. Scott and R.H. Holm, work in progress.
[84] X.-J. Lei, Z.-Y. Huang, M.-C. Hong, Q.-T. Liu and H.-Q. Liu, *Jiegou Huaxue, 9* (1990) 53.
[85] Z.-Y. Huang, X.-J. Lei, B.-S. Kang, J.-N. Liu, Q.-T. Liu, M.-C. Hong and H.-Q. Liu, *Inorg. Chim. Acta, 169* (1990) 25.
[86] A.L. Crumbliss, L.J. Gestaut, R.C. Rickard and A.T. McPhail, *J. Chem. Soc., Chem. Commun.,* (1974) 545.
[87] B.S. Snyder, M.S. Reynolds, I. Noda and R.H. Holm, *Inorg. Chem., 27* (1988) 595.
[88] B.S. Snyder and R.H. Holm, *Inorg. Chem., 27* (1988) 2339.
[89] M.S. Reynolds and R.H. Holm, *Inorg. Chem., 29* (1988) 4494.
[90] B.S. Snyder and R.H. Holm, *Inorg. Chem., 29* (1990) 274.
[91] D. Fenske and J. Ohmer, *Angew. Chem., Int. Ed. Engl., 26* (1987) 148.
[92] I. Noda, B.S. Snyder and R.H. Holm, *Inorg. Chem., 25* (1986) 3851.
[93] M.B. Power, J.W. Ziller and A.R. Barron, *Organometallics, 11* (1992) 2783.
[94] T. Krüger, B. Krebs and G. Henkel, *Angew. Chem., Int. Ed. Engl., 28* (1989) 61.
[95] J. El Nakat, K.J. Fisher, I.G. Dance and G.D. Willet, *Inorg. Chem., 32* (1993) 1931.
[96] Z. Yu, N. Zhang, X. Wu, Z. Gao, Q. Zhu and F. Kong, *J. Chem. Phys., 99* (1993) 1765.